Journal of the Mechanical Behavior of Biomedical Materials 173 (2026) 107222

Contents lists available at ScienceDirect

Journal of the Mechanical Behavior of Biomedical Materials

journal homepage: www.elsevier.com/locate/jmbbm

Biomechanical evaluation of shape-optimized CAD/CAM magnesium plates for mandibular reconstruction

Philipp Ruf [a,b], Kilian Richthofer [b], Vincenzo Orassi [b], Claudius Steffen [a], Georg N. Duda [b,c], Max Heiland [a], Sara Checa [b,d,*,1], Carsten Rendenbach [a,b,c,1]

[a] Department of Oral and Maxillofacial Surgery, Charité – Universitätsmedizin Berlin, Corporate Member of Freie Universität Berlin and Humboldt Universität zu Berlin, Augustenburger Platz 1, 13353, Berlin, Germany
[b] Julius Wolff Institute, Berlin Institute of Health at Charité - Universitätsmedizin Berlin, Augustenburger Platz 1, 13353, Berlin, Germany
[c] Berlin Institute of Health Center for Regenerative Therapies, Berlin Institute of Health at Charité - Universitätsmedizin Berlin, Augustenburger Platz 1, 13353, Berlin, Germany
[d] Institute of Biomechanics, Hamburg University of Technology (TUHH), Denickestrasse 15, 21073, Hamburg, Germany

ARTICLE INFO

Keywords:
Mandibular reconstruction
Finite element analysis
Magnesium
CAD/CAM miniplates
Shape-optimization
Biomechanics

ABSTRACT

Magnesium CAD/CAM miniplates are a promising alternative to titanium plates for mandibular reconstruction. However, gas formation is an inherent part of the magnesium degradation process, and thus, the quantity of magnesium used in fixation scenarios should be limited. Previous studies described several strategies to limit material volume, such as plate thickness reduction and shape-optimization. In particular, shape-optimization has been described as a strategy to limit material volume while maintaining mechanical integrity.

In consequence, the present study compared a shape-optimized CAD/CAM magnesium miniplate with standard CAD/CAM magnesium miniplates of varying thicknesses using a biomechanical finite element model. A single-segment mandibular reconstruction was chosen as the investigative scenario, evaluated under different biting tasks to assess the different plate shapes.

The shape-optimized magnesium plate demonstrated similar primary fixation stability compared to standard CAD/CAM magnesium miniplates, despite having reduced plate material and surface area. Shape optimization could help minimize magnesium volume and surface area to mitigate the issue of gas formation during the degradation process *in vivo* while maintaining biomechanical performance comparable to common CAD/CAM miniplates.

1. Introduction

Due to its degradability, excellent biocompatibility, reduced stiffness and reduced stress shielding, as well as reduced imaging artifacts in post-operative imaging, magnesium is a promising alternative to the gold-standard titanium for fracture fixation and free flap fixation in maxillofacial reconstruction (Espiritu et al., 2022; Filli et al., 2015; Rendenbach et al., 2018; Ruf et al., 2024; Wang et al., 2020; Schaller et al., 2018). However, the main limitation to the clinical use of magnesium plate osteosynthesis lies in its degradation behavior (Wang et al., 2020; Chaya et al., 2015; Fischer et al., 2022; Naujokat et al., 2020; Chakraborty Banerjee et al., 2019; Staiger et al., 2006; Witte, 2010; Zhao et al., 2017). As magnesium degrades, it produces gas, which can potentially lead to post-operative complications such as fistula formation, wound-healing disorders, or inflammation (Byun et al., 2020). The amount and rate of gas formation highly depends upon the volume and surface of the fixator (Naujokat et al., 2020; Chakraborty Banerjee et al., 2019; Rendenbach et al., 2021). Various approaches, such as alloying or surface modification, have been developed to slow the degradation process (Naujokat et al., 2020; Chakraborty Banerjee et al., 2019). However, these methods can only delay degradation and do not address the total amount of material implanted and thus the underlying cause of gas formation over time. In consequence, limiting the quantity of magnesium used in fixation devices remains the primary strategy for minimizing total gas formation that result in local accumulation of degradation products (Chakraborty Banerjee et al., 2019).

* Corresponding author. Augustenburger Platz 1, 13353, Berlin, Germany.
E-mail address: sara.checa@charite.de (S. Checa).
[1] These authors contributed equally to this work (co-last/equal authorship).

https://doi.org/10.1016/j.jmbbm.2025.107222
Received 15 March 2025; Received in revised form 23 September 2025; Accepted 4 October 2025
Available online 6 October 2025

Consequently, most studies have focused on evaluating magnesium in form of miniplates rather than larger reconstruction plates (Ruf et al., 2024; Fischer et al., 2022; Herzog et al., 2024; Orassi et al., 2021a; Turostowski et al., 2024).

Further strategies described in the literature to reduce the total material volume are plate thickness reduction or topology optimization (Fischer et al., 2022; Orassi et al., 2021a; Koper et al., 2021; Lang et al., 2021). While plate thickness reduction is a very simple approach, topology optimization is a sophisticated optimization strategy, in which a plate geometry is iteratively reshaped to minimize material volume and in-plate stress under a specific loading condition (Koper et al., 2021; Lang et al., 2021). In mandibular reconstruction, it has been shown that a topology optimized plate design consists of two parallel strands with a void in the middle (Koper et al., 2021; Lang et al., 2021). Therefore, this study aimed to biomechanically evaluate the potential of a shape-optimized magnesium CAD/CAM miniplate – whose design was inspired by the findings of the previous studies on topology optimization – compared to standard CAD/CAM magnesium miniplates of varying thickness. Finite element analyses of a one-segmental mandibular reconstruction using a fibula free flap were used as the primary method. The study evaluated mechanical stresses in the plates and mechanical strains in the healing regions.

2. Materials and methods

Existing finite element models of a reconstructed mandible with a single-segment fibula free flap were adapted to the present research question (Ruf et al., 2022, 2024).

2.1. Model geometry

The bony geometries were derived from a pre-operative CT scan of a 57-year-old female patient undergoing segmental mandibular resection due to oral squamous cell carcinoma with bone invasion. The CT scan was performed in axial mode with a slice thickness of 0.625 mm and a voxel size of 0.5 mm × 0.5 mm (General Electric, Boston, MA, USA). Image segmentation and meshing were conducted using Amira 6.0.1 (Thermo Fisher Scientific, Waltham, MA, USA), which differentiated cortical and trabecular bone in the mandible and fibula based on gray-scale values. Cortical bone was defined within Hounsfield Unit ranges of 300–2200 for the mandible and 250–2200 for the fibula, while trabecular bone and medullary spaces comprised the remaining inner areas.

In SolidWorks (2020) (Dassault Systèmes, Vélizy-Villacoublay, France), the virtual mandible resection and fibula placement were performed using a linearly extruded trapezoidal guide. The fibula segment measured 5 cm in length and 1.2 cm in diameter and was positioned from the right mandibular angle to the canine region.

In Abaqus CAE 2021 (Dassault Systèmes, Vélizy-Villacoublay, France), the mandible and fibula geometries were integrated into a single volume part with four subdivided geometry sets. Intersegmental gaps were created at the resection interfaces to represent regions of interest (ROIs) for evaluating mechanical strains. A gap width of 1 mm was chosen to simulate a realistic scenario (Steffen et al., 2022; Hashemi et al., 2020).

2.2. Fixation scenarios

Since previous studies have identified the anterior healing region as a potential area for the use of magnesium plates (Ruf et al., 2024; Orassi et al., 2021a), three different magnesium CAD/CAM miniplate designs were tested in the anterior region, paired with a short 2.0 mm CAD/CAM titanium reconstruction plate in the posterior region. All miniplate designs were created using 3matic (Materialise, Leuven, Belgium) in collaboration with the senior author and according to clinical standards. A standardized distance of the first screw to the osteotomy of 5 mm was defined to reduce the impact of screw placement on primary fixation stability (Li et al., 2024). According to previous studies, paired 1.0 or 1.5 mm thick standard CAD/CAM magnesium miniplates were investigated (Fischer et al., 2022; Orassi et al., 2021a) (Fig. 1). In addition, a shape-optimized plate of 1.5 mm thickness with 3 screws on each side of the osteotomy was created with a partially void bridge, in line with previous studies on topology optimization (Koper et al., 2021; Lang et al., 2021). The two strands of the bridge are each 2.3 mm wide with a 1.5 mm gap in between (Fig. 1). Monocortical magnesium screws (7 mm length and 2 mm diameter) of simplified geometry were employed in all screw holes in the CAD/CAM miniplates and the shape-optimized plate (Ruf et al., 2022, 2024; Steffen et al., 2020). The lengths of the screws fixing the reconstruction plate to the fibula were 7 mm to prevent harm to the interosseous vessels (Steffen et al., 2020). In the mandibular angle region, the reconstruction plate was fixed bicortically with screw lengths of 7–8 mm.

2.3. Meshing and convergence

All geometries were meshed in Abaqus CAE 2021 using second-order (quadratic) tetrahedral elements. Mesh sizes of 0.2 mm in the healing regions, 0.25 mm for the plates, and 1.0 mm for the screws were employed. Mesh convergence results from a prior study were considered valid for the present study (Ruf et al., 2022).

2.4. Boundary conditions and loading

Tie constraints were used to simulate the connection of the screws, plates, and bone tissue. For unilateral and incisal biting simulations, the premolars and first molars (unilateral) and the incisors (incisal) were restricted from vertical displacement, and condyles were fixed in the glenoid fossa. Main biting muscles, including the masseter, temporalis, and pterygoid, were modeled as loads. Muscle forces and activations were adapted (full detachment of the superficial masseter and 50 % detachment of the deep masseter on the resection side) from the literature and scaled to 12.5 % to simulate post-operative conditions, resulting in a 45 N bite force under unilateral biting (Ruf et al., 2022; Korioth and Hannam, 1994; Korioth et al., 1992; Lovald et al., 2009). This value is in line with previously reported postoperative measurements 2 weeks after fracture reposition (Gheibollahi et al., 2021). The exact muscle insertion areas, fiber activations, muscle directions and muscle forces have been described in previous studies (Ruf et al., 2022, 2024) and can be found in Appendix 1.

2.5. Material properties

Cortical bone was considered as anisotropic, linear-elastic material, while isotropic linear-elastic properties were used for trabecular bone, dentine, granulation tissue, and fixation systems. Granulation tissue filled the interosseous gaps and fibula medullary spaces. Titanium Ti6Al4V and magnesium WE43 material properties were defined, with yield stresses of 830 MPa and 162 MPa, respectively, used as thresholds for material failure (MatWeb, 2024a, 2024b). The material properties were derived from the literature (Ruf et al., 2024; Korioth and Hannam, 1994; Lovald et al., 2009; MatWeb, 2024a, 2024b; Lefèvre et al., 2015; Rho, 1996; Schwartz-Dabney and Dechow, 2003; Lakatos et al., 2014; Leong and Morgan, 2008) and are presented in Appendix 2.

2.6. Output evaluation

Mechanical maximum and minimum principal strains within the healing regions were analyzed as indicators of potential healing outcomes. Only elements with absolute strains exceeding 500 μstrain were included in the evaluation to minimize the influence of elements that are not part of the direct interface of the different-sized bones mandible and fibula on the results. Using this elimination operation, the comparison between strain percentiles of the different-sized anterior and posterior

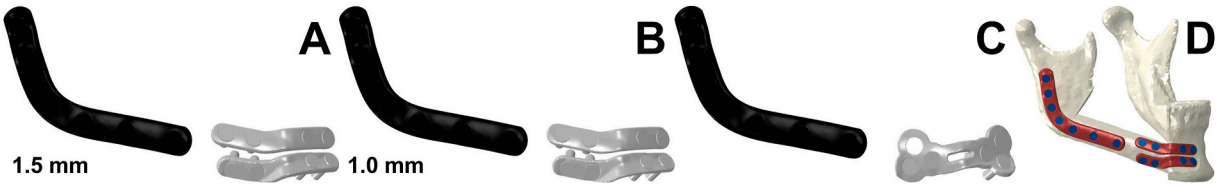

Fig. 1. – Investigated fixation scenarios including the 1.5 mm thick miniplates (A), the 1.0 mm thick miniplates (B) and the shape-optimized plate (C); exemplary illustration of the plate fixation on the mandible (D).

gaps is feasible. Remaining outlier values were eliminated using the ROUT-method (Q = 0.1 %) (Motulsky and Brown, 2006). Peak von Mises stresses in the plates were calculated and compared to material yield strengths to assess failure risks. Stress singularities due to model constraints were minimized by excluding the top 0.01 % and averaging the 10 greatest of the remaining values.

3. Results

The 1.5 mm miniplates had a combined volume of 417 mm^3 and a screw volume of 288 mm^3, resulting in a total magnesium volume of 705 mm^3. The 1.0 mm miniplates had a combined plate volume of 272 mm^3, leading to a total magnesium volume of 560 mm^3, which represents a 21 % reduction compared to the 1.5 mm miniplates. The shape-optimized plate, with a 1.5 mm thickness, had a volume of 328 mm^3, with a screw volume of 216 mm^3, resulting in a total magnesium volume of 544 mm^3 - a 23 % reduction compared to the 1.5 mm miniplates.

Additionally, the bridge region was assessed separately, as it is considered the most critical area for primary fixation stability. The 1.5 mm thick miniplates had a bridge volume of 144 mm^3, while the 1.0 mm miniplates had a bridge volume of 97 mm^3 - a 33 % reduction compared to the 1.5 mm plates. The shape-optimized plate had a bridge volume of 73 mm^3, which represented a 49 % reduction compared to the 1.5 mm thick miniplates.

The 1.5 mm thick miniplates had a combined surface area of 838 mm^2 and their screws 597 mm^2, resulting in a total surface of 1435 mm^2. The 1.0 mm miniplates had a combined surface area of 740 mm^2, resulting in a total surface of 1337 mm^2 - a 7 % reduction compared to the 1.5 mm miniplates. The shape-optimized plate had a surface of 644 mm^2 and its screws of 453 mm^2, the total surface was 1097 mm^2 - a 24 % reduction compared to the 1.5 mm miniplates.

The boundary and loading conditions resulted in bite forces ranging from 11 N to 11.5 N for incisal biting and 44 N–44.5 N for unilateral biting across the different plating scenarios.

3.1. A shape-optimized magnesium miniplate induces similar mechanical stimuli within the healing region compared with standard magnesium miniplates

Qualitative and quantitative strain levels are presented in Fig. 2. Posterior strain levels were highly dependent on the biting scenario, with unilateral biting (percentiles for scenarios 1.5 mm thick miniplates: 0.25–0.2 %, 0.5–0.29 %, 0.75–0.53 %, 1–1.35 %; 1.0 mm thick miniplates: 0.25–0.19 %, 0.5–0.28 %, 0.75–0.52 %, 1–1.32 %; shape-optimized plate: 0.25–0.19 %, 0.5–0.28 %, 0.75–0.52 %, 1–1.33 %) inducing higher strains in the posterior region compared to incisal biting (percentiles for scenarios 1.5 mm thick miniplates: 0.25–0.12 %, 0.5–0.16 %, 0.75–0.29 %, 1–0.61 %; 1.0 mm thick miniplates: 0.25–0.11 %, 0.5–0.15 %, 0.75–0.27 %, 1–0.56 %; shape-optimized plate: 0.25–0.11 %, 0.5–0.15 %, 0.75–0.27 %, 1–0.55 %). In the anterior region, unilateral biting (percentiles for scenarios 1.5 mm thick miniplates: 0.25–0.21 %, 0.5–0.38 %, 0.75–0.49 %, 1–1.32 %; 1.0 mm

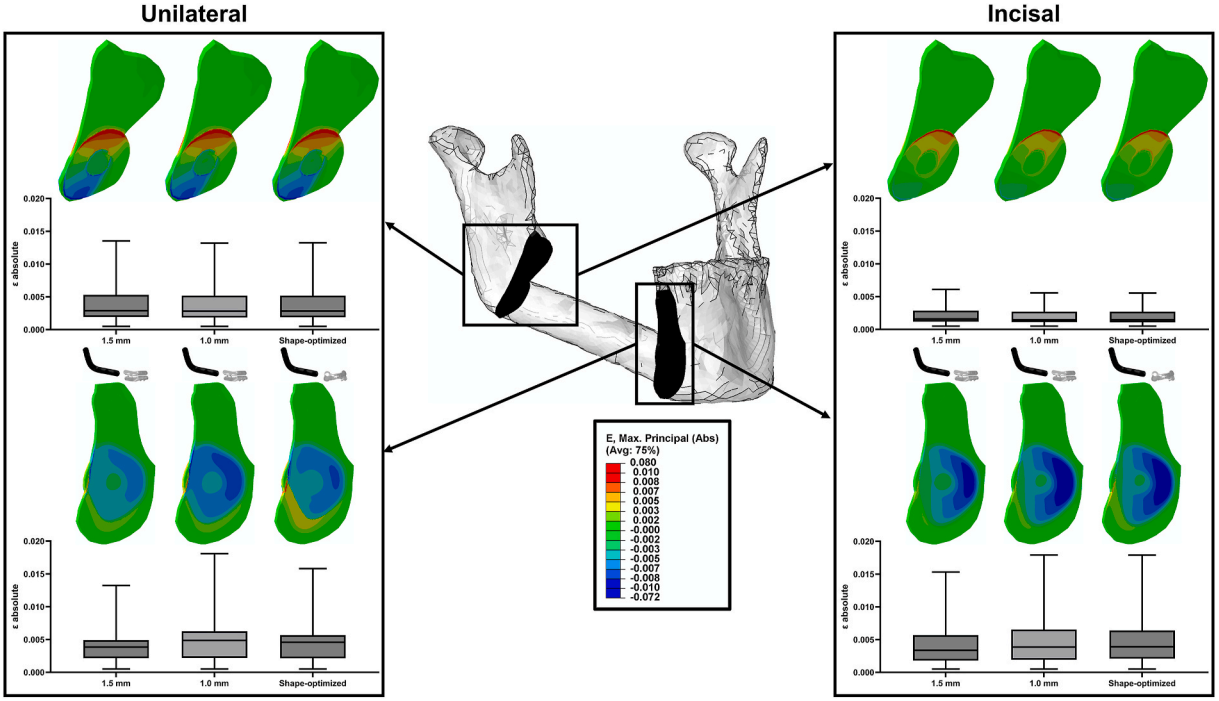

Fig. 2. – Intersegmental strain distributions in box plots (percentiles 0.75, 0.5 and 0.25) and contour plots for the anterior (bottom) and posterior (top) intersegmental gaps under unilateral (left) and incisal biting (right) over the investigated plating scenarios.

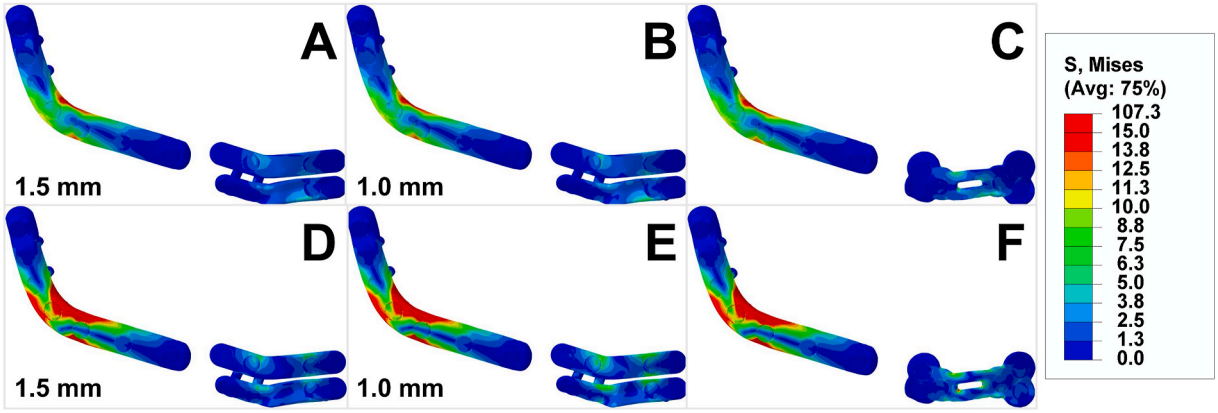

Fig. 3. – Contour plots of von Mises stress (Legend in MPa) in the plates including the 1.5 mm thick magnesium plates (A, D), the 1.0 mm thick magnesium plates (B, E) and the shape-optimized plate (C, F) under the biting scenarios of incisal (A–C) and unilateral biting (D–F).

thick miniplates: 0.25–0.22 %, 0.5–0.49 %, 0.75–0.62 %, 1–1.81 %; shape-optimized plate: 0.25–0.21 %, 0.5–0.46 %, 0.75–0.57 %, 1–1.58 %) and incisal biting (percentiles for scenarios 1.5 mm thick miniplates: 0.25–0.18 %, 0.5–0.34 %, 0.75–0.57 %, 1–1.53 %; 1.0 mm thick miniplates: 0.25–0.19 %, 0.5–0.39 %, 0.75–0.65 %, 1–1.79 %; shape-optimized plate: 0.25–0.21 %, 0.5–0.39 %, 0.75–0.64 %, 1–1.79 %) produced similar strain levels, which were comparable to posterior strain levels under unilateral biting.

The variation in the anterior magnesium plates did not greatly influence anterior strain levels across the scenarios. Only the 1.5 mm thick miniplate slightly reduced the local intersegmental strain compared to the other two configurations. In addition, the changes in anterior fixation geometry had no effect on posterior strain levels for any of the biting scenarios.

3.2. Maximum stresses in the shape-optimized plate are comparable to those induced in standard magnesium miniplates

The contour plots of the von Mises stresses in the plates are presented in Fig. 3. The maximum stress values for each plate, along with the relative stresses (calculated as the ratio of maximum stress to the material's yield stress), are detailed in Table 1 for incisal biting and Table 2 for unilateral biting.

Higher stresses in the plates were observed during unilateral biting compared to incisal biting. The highest absolute stress was located in the mandibular angle region of the titanium reconstruction plate, reaching 19 MPa during incisal biting and 39 MPa during unilateral biting. The design variation in the anterior miniplates plates did not influence the stress levels in the posterior titanium reconstruction plate.

In the standard miniplates and the shape-optimized plate, stress peaks were concentrated in the bridge region (Fig. 3). In the anterior region, similar maximum stresses were observed in the shape-optimized plate (8 MPa for incisal biting and 14 MPa for unilateral biting) and the 1.0 mm thick miniplates (8 MPa under incisal biting and 13 MPa under unilateral biting). The 1.5 mm thick standard miniplates experienced maximum stresses of 7 MPa during incisal biting and 10 MPa during unilateral biting.

When comparing the two materials, the magnesium plates exhibited higher relative stress values (defined as the percentage of maximum stress relative to the material's yield stress) than the titanium reconstruction plate. The maximum relative stress was 8.5 % for the shape-optimized plate under unilateral biting. In contrast, the titanium reconstruction plate experienced only 4.7 % of its yield stress during unilateral biting.

4. Discussion

Magnesium is considered a potential alternative to titanium for mandibular reconstruction due to its degradability, reduced imaging artifacts, and lower stiffness compared to titanium (Espiritu et al., 2022;

Table 1
Maximum stress values and maximum relative stress values (% of yield stresses: 830 MPa for titanium and 162 MPa for magnesium) in the investigated plating scenarios under incisal biting.

		1.5 mm thick miniplates	1.0 mm thick miniplates	Shape-optimized plate
	posterior reconstruction plate	18.9 MPa (2.3 %)	18.8 MPa (2.3 %)	18.7 MPa (2.3 %)
anterior	superior miniplate	6.4 MPa (3.9 %)	7.9 MPa (4.9 %)	8.1 MPa (5 %)
	inferior miniplate	7 MPa (4.3 %)	7.6 MPa (4.7 %)	

Table 2
Maximum stress values and maximum relative stress (% of yield stresses: 830 MPa for titanium and 162 MPa for magnesium) values in the investigated plating scenarios under unilateral biting.

		1.5 mm thick miniplates	1.0 mm thick miniplates	Shape-optimized plate
	posterior reconstruction plate	39 MPa (4.7 %)	38.5 MPa (4.6 %)	38.7 MPa (4.7 %)
anterior	superior miniplate	10.1 MPa (6.2 %)	13.2 MPa (8.2 %)	13.8 MPa (8.5 %)
	inferior miniplate	8.5 MPa (5.2 %)	12.8 MPa (7.9 %)	

Filli et al., 2015; Rendenbach et al., 2018; Ruf et al., 2024; Wang et al., 2020; Chakraborty Banerjee et al., 2019; Staiger et al., 2006; Witte, 2010; Zhao et al., 2017; Turostowski et al., 2024). However, a major limitation to the use of magnesium is the gas formation during degradation, which is directly proportional to the amount of magnesium material (Chakraborty Banerjee et al., 2019). Therefore, the present study aimed to biomechanically evaluate the possibility of magnesium material reduction by reduced plate thickness and optimized shape design. It was shown that plate material reduction in the anterior areas by shape-optimization resulted in similar biomechanical conditions compared to 1.0 mm thick magnesium miniplates and 1.5 mm thick magnesium miniplates.

Previously, two parallel magnesium plates with the thickness of 1.5 mm have been shown to provide sufficient primary fixation stability as they were assessed as equally stable compared to clinically used 1.0 mm titanium miniplates (Fischer et al., 2022). This biomechanical *in vitro* test has been performed on sheep mandibles as sheep mandibles provide a similar biomechanical environment in comparison to human mandibles (Fischer et al., 2022; Orassi et al., 2021b). 1.0 mm magnesium miniplates have been assessed *in silico* showing acceptable stresses compared to 1.5 mm magnesium miniplates and 1.0 mm titanium miniplates particularly in the anterior areas (Orassi et al., 2021a). Thus, the present study is in line with the previous studies as similar stresses have been found when comparing the 1.0 mm magnesium miniplates and the 1.5 mm magnesium miniplates in the anterior areas. The newly designed shape-optimized plate showed similar maximum stress values compared to the two investigated magnesium miniplate configurations.

The corpus/symphysis interface region of the reconstructed mandible has been shown to be a good fit for magnesium plates since they can increase the biomechanical stimuli in this critical region in comparison to titanium plates and subsequently enhance bone formation (Ruf et al., 2022, 2024; Steffen et al., 2022). Magnesium's degradability is particularly advantageous in the anterior regions, as non-degradable titanium plates often require removal prior to dental rehabilitation of the tooth-bearing region (Ruf et al., 2024; Kreutzer et al., 2022). In consequence, the present study investigated the shape-optimized magnesium plate in the anterior region. Analogously to the previous studies, similar primary fixation stabilities of magnesium miniplates of varying thicknesses have been observed (Fischer et al., 2022; Orassi et al., 2021a). In this study, the shape-optimized magnesium plate was shown to provide similar fixation stability as the magnesium miniplates, with a relevant reduction in material volume, particularly in the crucial bridge area. Furthermore, the surface area has been reduced by shape-optimization. Plate topology-optimization has been performed for mandible reconstruction cases in previous studies. The resulting plate shape showed two parallel plate strands as bridge between the screw holes and has served as model for the shape-optimized plate in the present study (Koper et al., 2021; Lang et al., 2021). In consequence, the present study sides with the previous studies in recommending shape-optimized magnesium plates in the anterior areas for mandibular reconstruction.

Because gas formation limits magnesium's clinical application, approaches to reducing gas generation are critical (Chakraborty Banerjee et al., 2019). While surface modifications can slow degradation, this strategy merely delays gas formation rather than reducing its total quantity (Naujokat et al., 2020; Chakraborty Banerjee et al., 2019; Rendenbach et al., 2021; Kopp et al., 2019, 2022). In contrast, limiting magnesium material through techniques like shape-optimization or plath thickness reduction reduces the absolute amount of gas produced, offering a more effective solution (Chakraborty Banerjee et al., 2019). Within the present study, shape optimization has resulted in a 23 % material reduction compared to the 1.5 mm thick miniplates while maintaining the mechanical integrity. The mechanically particularly relevant bridge area experienced a material reduction of 49 % comparing the 1.5 mm thick miniplates to the shape optimized plate. The reason for the particular material reduction in the bridge area was that 3 screws were employed on each side of the shape-optimized plate - a limitation to the material reduction in these areas. However, in addition to the volume reduction, the shape-optimized plate presented a further surface reduction of 24 % in comparison to the 1.5 mm miniplates.

Delayed osseous union and pseudarthrosis are common challenges in mandibular reconstruction (Knitschke et al., 2022a, 2022b; Rendenbach et al., 2019). Intersegmental strain is a key stimulus for bone formation, especially during the critical initial healing phase (Duda et al., 2023). Studies on one-segmental mandibular reconstructions have shown that patient-specific reconstruction plates achieve favorable healing outcomes in the posterior regions (Steffen et al., 2022). In both the present study and prior research, anterior magnesium miniplates plates induced strain levels in the anterior regions comparable to those in posterior regions under reconstruction plate fixation (interquartile ranges from quartiles 0.25 to 0.75 under unilateral biting of 0.2 %–0.6 % in the anterior and 0.2 %–0.5 % in the posterior intersegmental gap) (Ruf et al., 2024). This suggests that localized application of anterior magnesium miniplates or shape-optimized plates could enhance bone formation in reconstructed mandibles.

The anatomy of the human mandible has been described has highly variable between individuals (Puisoru et al., 2006). Therefore, it can be considered a limitation of the present study that only one patient was investigated within the present study. However, within the present study, on purpose, only one patient has been investigated with different plating scenarios to eliminate the influence of anatomical variability on biomechanical results. Nevertheless, future studies should incorporate multiple patients to validate the biomechanical findings across different anatomical setups. Possible anatomical factors influencing the primary fixation stability could be mandible shape, bone density or cortical thickness.

Technically, shape optimization is limited to patient-specific plates. Magnesium WE43 exhibits a narrow plastic phase, with an elongation at break of just 2 % compared to 28 % for pure titanium (MatWeb, 2024a, 2024c). This characteristic makes magnesium unsuitable for pre-bending and restricts its use to fixations that do not require permanent plate deformation. In a previous *in vitro* study comparing magnesium and titanium miniplates, plate failure patterns correlated with the varying material properties: Pure titanium plates failed due to abnormal deformation, whereas magnesium plates showed a brittle failure mechanism without visible plastic deformation around failure points (Fischer et al., 2022). As a result, magnesium plates generally require patient-specific production, which aligns well with shape optimization techniques.

Although the initial healing phase has been shown to be crucial for bone formation, bone healing is a process of many stages (Duda et al., 2023; Claes, 2017a, 2017b; Claes and Heigele, 1999). In this study, we focused on initial mechanical stability. Future studies are needed to investigate the role of mechanical conditions induced by magnesium miniplates on the later stages of the bone regeneration process.

To conclude, shape-optimization of magnesium miniplates appears an effective strategy for reducing material usage while preserving primary fixation stability for mandibular reconstruction. For magnesium miniplates, material reduction is of particular relevance because degradation and gas formation are the primary limitations to their clinical application. Shape-optimized plates provide a promising solution for enabling the clinical use of magnesium in mandibular reconstruction.

CRediT authorship contribution statement

Philipp Ruf: Writing – review & editing, Writing – original draft, Visualization, Validation, Software, Methodology, Investigation, Formal analysis, Data curation, Conceptualization. **Kilian Richthofer:** Writing – review & editing, Software, Methodology, Data curation. **Vincenzo Orassi:** Writing – review & editing, Methodology, Investigation.

Claudius Steffen: Validation, Data curation. **Georg N. Duda:** Writing – review & editing, Supervision, Resources. **Max Heiland:** Writing – review & editing, Supervision, Resources, Project administration, Funding acquisition. **Sara Checa:** Writing – original draft, Supervision, Resources, Project administration, Methodology, Funding acquisition, Conceptualization. **Carsten Rendenbach:** Writing – original draft, Supervision, Resources, Project administration, Funding acquisition, Conceptualization.

Declaration of generative AI and AI-assisted technologies in the writing process

During the preparation of this work the authors used ChatGPT (OpenAI Inc., San Francisco, United States) in order to check grammar and spelling and improve the readability of the article. After using this tool, the authors reviewed and edited the content as needed and take full responsibility for the content of the publication.

Declaration of competing interest

Max Heiland received speaker remuneration and research funding for other projects by KLS Martin SE & Co. KG. Carsten Rendenbach received research funding for other projects by KLS Martin SE & Co. KG.

Acknowledgements

The authors acknowledge the support of the European Union (EU) Horizon 2020 for the project InterLynk (grant agreement: H2020-NMBP-TR-IND-2020, project ID: 953169). This study was partially funded by the German Research Foundation (Deutsche Forschungsgemeinschaft CH 1123/10-1 and RE 4803/1-1). The authors acknowledge the support of Clarence Janka, Adem Aksu and Frank Reinauer from KLS Martin SE & Co. KG, in design consulting regarding the patient-specific plates.

Appendix

Appendix 1 - Healthy maximum muscle forces, reduced maximum muscle forces on 12.5 %, fiber directions and fiber activations for the participating muscles in the investigated biting tasks unilateral (UNI) and incisal (INC) biting; fiber direction definition relative to the frontal (XY), transversal (XZ), and sagittal (YZ) planes

	Healthy Maximum Muscle Force (N)	12,5 % of Maximum Muscle Force (N)	Fiber direction				Fiber activation			
			X		Y	Z	INC		UNI	
			Right	Left			Right	Left	Right	Left
Superficial Masseter	190,4	23,8	−0,207	0,207	0,884	0,419	0	0,4	0	0,72
Deep Masseter	81,6	10,2	−0,546	0,546	0,758	−0,358	0,13	0,26	0,3	0,72
Medial Pterygoid	174,8	21,85	0,486	−0,486	0,791	0,373	0,78	0,78	0,6	0,84
Lateral Pterygoid	66,9	8,3625	0,63	−0,63	−0,174	0,757	0,71	0,71	0,65	0,3
Anterior Temporalis	158	19,75	−0,149	0,149	0,988	0,044	0,08	0,08	0,58	0,73
Middle Temporalis	95,6	11,95	−0,222	0,222	0,837	−0,5	0,06	0,06	0,67	0,66
Posterior Temporalis	75,6	9,45	−0,208	0,208	0,474	−0,855	0,04	0,04	0,39	0,59

Appendix 2 - Anisotropic and isotropic material properties for bone, intersegmental gaps, and fixation materials. 1: longitudinal; 2: tangential; 3: transverse

Material	Symphysis	Body	Angle	Ramus	Condyle	Coronoid	Fibula cortical	Dentin	Mandible trabecular	Granulation Tissue	Ti-6AI-4V	WE43
E1 (MPa)	20492	21728	23793	24607	23500	28000	28000	17600	300	1	114000	44200
E2 (MPa)	16350	17828	19014	18357	17850	17500	17700	17600	300	1	114000	44200
E3 (MPa)	12092	12700	12757	12971	12650	14000	17700	17600	300	1	114000	44200
Nu12	0,34	0,34	0,3	0,28	0,24	0,23	0,237	0,34	0,3	0,3	0,33	0,27
Nu23	0,22	0,2	0,22	0,23	0,25	0,28	0,42	0,34	0,3	0,3	0,33	0,27
Nu13	0,43	0,45	0,41	0,38	0,32	0,28	0.231	0,34	0,3	0,3	0,33	0,27
G12 (MPa)	6908	7450	7579	7407	7150	7150	4690	6567	115,4	0,385	44000	17000
G23 (MPa)	4825	5083	4986	5014	5150	5300	3600	6567	115,4	0,385	44000	17000
G13 (MPa)	5317	5533	5493	5386	5500	5750	4720	6567	115,4	0,385	44000	17000

Data availability

Data will be made available on request.

References

Byun, S.-H., Lim, H.-K., Cheon, K.-H., Lee, S.-M., Kim, H.-E., Lee, J.-H., 2020. Biodegradable magnesium alloy (WE43) in bone-fixation plate and screw. Journal of biomedical materials research. Part B, Applied biomaterials 108 (6), 2505–2512.

Chakraborty Banerjee, P., Al-Saadi, S., Choudhary, L., Harandi, S.E., Singh, R., 2019. Magnesium implants: prospects and challenges. Materials 12 (1).

Chaya, A., Yoshizawa, S., Verdelis, K., Myers, N., Costello, B.J., Chou, D.-T., Pal, S., Maiti, S., Kumta, P.N., Sfeir, C., 2015. In vivo study of magnesium plate and screw degradation and bone fracture healing. Acta Biomater. 18, 262–269.

Claes, L., 2017a. [Mechanobiology of fracture healing part 2 : relevance for internal fixation of fractures]. Unfallchirurg 120 (1), 23–31.
Claes, L., 2017b. [Mechanobiology of fracture healing part 1 : Principles]. Unfallchirurg 120 (1), 14–22.
Claes, L.E., Heigele, C.A., 1999. Magnitudes of local stress and strain along bony surfaces predict the course and type of fracture healing. J. Biomech. 32 (3), 255–266.
Duda, G.N., Geissler, S., Checa, S., Tsitsilonis, S., Petersen, A., Schmidt-Bleek, K., 2023. The decisive early phase of bone regeneration. Nat. Rev. Rheumatol. 19, 78–95.
Espiritu, J., Berangi, M., Yiannakou, C., Silva, E., Francischello, R., Kuehne, A., Niendorf, T., Konneker, S., Willumeit-Romer, R., Seitz, J.M., 2022. Evaluating metallic artefact of biodegradable magnesium-based implants in magnetic resonance imaging. Bioact. Mater. 15, 382–391.
Filli, L., Luechinger, R., Frauenfelder, T., Beck, S., Guggenberger, R., Farshad-Amacker, N., Andreisek, G., 2015. Metal-induced artifacts in computed tomography and magnetic resonance imaging: comparison of a biodegradable magnesium alloy versus titanium and stainless steel controls. Skelet. Radiol. 44 (6), 849–856.
Fischer, H., Schmidt-Bleek, O., Orassi, V., Wulsten, D., Schmidt-Bleek, K., Heiland, M., Steffen, C., Rendenbach, C., 2022. Biomechanical comparison of WE43-Based magnesium vs. titanium miniplates in a mandible fracture model in sheep. Materials 16 (1).
Gheibollahi, H., Aliabadi, E., Khaghaninejad, M.S., Mousavi, S., Babaei, A., 2021. Evaluation of bite force recovery in patients with maxillofacial fracture. Journal of cranio-maxillo-facial surgery : official publication of the European Association for Cranio-Maxillo-Facial Surgery.
Hashemi, S., Oda, M., Onoue, K., Basa, K., Rubin, S.J., Sakai, O., Salama, A., Ezzat, W.H., 2020. Determining the optimal osteotomy distance with the fibula free flap in mandibular reconstruction. Am. J. Otolaryngol. 41 (3), 102436.
Herzog, P., Rendenbach, C., Turostowski, M., Ellinghaus, A., Prates Soares, A., Heiland, M., Duda, G.N., Schmidt-Bleek, K., Fischer, H., 2024. Titanium versus plasma electrolytic oxidation surface-modified magnesium miniplates in a forehead secondary fracture healing model in sheep. Acta Biomater. 185, 98–110.
Knitschke, M., Sonnabend, S., Roller, F.C., Pons-Kühnemann, J., Schmermund, D., Attia, S., Streckbein, P., Howaldt, H.-P., Böttger, S., 2022a. Osseous union after mandible reconstruction with Fibula free flap using manually bent plates vs. patient-specific implants: a retrospective analysis of 89 patients. Curr. Oncol. 29 (5), 3375–3392.
Knitschke, M., Yonan, M., Roller, F.C., Pons-Kühnemann, J., Attia, S., Howaldt, H.-P., Streckbein, P., Böttger, S., 2022b. Osseous union after jaw reconstruction with fibula-free flap: conventional vs. CAD/CAM patient-specific implants. Cancers 14 (23).
Koper, D.C., Leung, C.A.W., Smeets, L.C.P., Laeven, P.F.J., Tuijthof, G.J.M., Kessler, P., 2021. Topology optimization of a mandibular reconstruction plate and biomechanical validation. J. Mech. Behav. Biomed. Mater. 113, 104157.
Kopp, A., Derra, T., Müther, M., Jauer, L., Schleifenbaum, J.H., Voshage, M., Jung, O., Smeets, R., Kröger, N., 2019. Influence of design and postprocessing parameters on the degradation behavior and mechanical properties of additively manufactured magnesium scaffolds. Acta Biomater. 98, 23–35.
Kopp, A., Fischer, H., Soares, A.P., Schmidt-Bleek, K., Leber, C., Kreiker, H., Duda, G., Kröger, N., van Gaalen, K., Hanken, H., Jung, O., Smeets, R., Heiland, M., Rendenbach, C., 2022. Long-term in vivo observations show biocompatibility and performance of ZX00 magnesium screws surface-modified by plasma-electrolytic oxidation in Göttingen miniature pigs. Acta Biomater. 157, 720–733.
Korioth, T.W., Hannam, A.G., 1994. Deformation of the human mandible during simulated tooth clenching. J. Dent. Res. 73 (1), 56–66.
Korioth, T.W., Romilly, D.P., Hannam, A.G., 1992. Three-dimensional finite element stress analysis of the dentate human mandible. Am. J. Phys. Anthropol. 88 (1), 69–96.
Kreutzer, K., Steffen, C., Nahles, S., Koerdt, S., Heiland, M., Rendenbach, C., Beck-Broichsitter, B., 2022. Removal of patient-specific reconstruction plates after mandible reconstruction with a fibula free flap: is the plate the problem? Int. J. Oral Maxillofac. Surg. 51 (2), 182–190.
Lakatos, É., Magyar, L., Bojtár, I., 2014. Material properties of the mandibular trabecular bone. Journal of medical engineering 2014, 470539.
Lang, J.J., Bastian, M., Foehr, P., Seebach, M., Weitz, J., von Deimling, C., Schwaiger, B. J., Micheler, C.M., Wilhelm, N.J., Grosse, C.U., Kesting, M., Burgkart, R., 2021. Improving mandibular reconstruction by using topology optimization, patient specific design and additive manufacturing?-A biomechanical comparison against miniplates on human specimen. PLoS One 16 (6), e0253002.
Lefèvre, E., Lasaygues, P., Baron, C., Payan, C., Launay, F., Follet, H., Pithioux, M., 2015. Analyzing the anisotropic Hooke's law for children's cortical bone. J. Mech. Behav. Biomed. Mater. 49, 370–377.
Leong, P.L., Morgan, E.F., 2008. Measurement of fracture callus material properties via nanoindentation. Acta Biomater. 4 (5), 1569–1575.
Li, Z., Pollard, S., Smith, G., Deshmukh, S., Ding, Z., 2024. Biomechanical analysis of combi-hole locking compression plate during fracture healing: a numerical study of screw configuration. Proc. Inst. Mech. Eng. H 238 (3), 313–323.
Lovald, S.T., Wagner, J.D., Baack, B., 2009. Biomechanical optimization of bone plates used in rigid fixation of mandibular fractures. Journal of oral and maxillofacial surgery : official journal of the American Association of Oral and Maxillofacial Surgeons 67 (5), 973–985.
MatWeb, 2024a. Material property data: magnesium WE43-T6, cast. https://www.matweb.com/search/datasheet.aspx?matguid=4b8a8c13cf354fc5893a40cf8eca022c&ckck=1. (Accessed 23 September 2024).
MatWeb, 2024b. Titanium Ti-6Al-4V (Grade 5), Annealed bar. https://www.matweb.com/search/DataSheet.aspx?MatGUID=10d463eb3d3d4ff48fc57e0ad1037434. (Accessed 19 June 2024).
MatWeb, 2024c. Titanium grade 2, annealed. https://www.matweb.com/search/datasheet.aspx?MatGUID=49a4b764217b44ee953205822af5fbc9. (Accessed 19 June 2024).
Motulsky, H.J., Brown, R.E., 2006. Detecting outliers when fitting data with nonlinear regression - a new method based on robust nonlinear regression and the false discovery rate. BMC Bioinf. 7, 123.
Naujokat, H., Ruff, C.B., Kluter, T., Seitz, J.M., Acil, Y., Wiltfang, J., 2020. Influence of surface modifications on the degradation of standard-sized magnesium plates and healing of mandibular osteotomies in miniature pigs. Int. J. Oral Maxillofac. Surg. 49 (2), 272–283.
Orassi, V., Fischer, H., Duda, G.N., Heiland, M., Checa, S., Rendenbach, C., 2021a. In silico biomechanical evaluation of WE43 magnesium plates for Mandibular Fracture fixation. Front. Bioeng. Biotechnol. 9, 803103.
Orassi, V., Duda, G.N., Heiland, M., Fischer, H., Rendenbach, C., Checa, S., 2021b. Biomechanical assessment of the validity of sheep as a preclinical model for testing mandibular fracture fixation devices. Front. Bioeng. Biotechnol. 9, 672176.
Puisoru, M., Forna, N., Fatu, A.M., Fatu, R., Fatu, C., 2006. Analysis of mandibular variability in humans of different geographic areas. Ann. Anat. 188 (6), 547–554.
Rendenbach, C., Schoellchen, M., Bueschel, J., Gauer, T., Sedlacik, J., Kutzner, D., Vallittu, P.K., Heiland, M., Smeets, R., Fiehler, J., Siemonsen, S., 2018. Evaluation and reduction of magnetic resonance imaging artefacts induced by distinct plates for osseous fixation: an in vitro study @ 3 T. Dentomaxillofacial Radiol. 47 (7), 20170361.
Rendenbach, C., Steffen, C., Hanken, H., Schluermann, K., Henningsen, A., Beck-Broichsitter, B., Kreutzer, K., Heiland, M., Precht, C., 2019. Complication rates and clinical outcomes of osseous free flaps: a retrospective comparison of CAD/CAM versus conventional fixation in 128 patients. Int. J. Oral Maxillofac. Surg. 48 (9), 1156–1162.
Rendenbach, C., Fischer, H., Kopp, A., Schmidt-Bleek, K., Kreiker, H., Stumpp, S., Thiele, M., Duda, G., Hanken, H., Beck-Broichsitter, B., Jung, O., Kröger, N., Smeets, R., Heiland, M., 2021. Improved in vivo osseointegration and degradation behavior of PEO surface-modified WE43 magnesium plates and screws after 6 and 12 months, materials science & engineering. C, Materials for biological applications 129, 112380.
Rho, J.Y., 1996. An ultrasonic method for measuring the elastic properties of human tibial cortical and cancellous bone. Ultrasonics 34 (8), 777–783.
Ruf, P., Orassi, V., Fischer, H., Steffen, C., Duda, G.N., Heiland, M., Kreutzer, K., Checa, S., Rendenbach, C., 2022. Towards mechanobiologically optimized mandible reconstruction: CAD/CAM miniplates vs. reconstruction plates for fibula free flap fixation: a finite element study. Front. Bioeng. Biotechnol. 10.
Ruf, P., Orassi, V., Fischer, H., Steffen, C., Kreutzer, K., Duda, G.N., Heiland, M., Checa, S., Rendenbach, C., 2024. Biomechanical evaluation of CAD/CAM magnesium miniplates as a fixation strategy for the treatment of segmental mandibular reconstruction with a fibula free flap. Comput. Biol. Med. 168, 107817.
Schaller, B., Matthias Burkhard, J.P., Chagnon, M., Beck, S., Imwinkelried, T., Assad, M., 2018. Fracture healing and bone remodeling with human standard-sized magnesium versus polylactide-co-glycolide plate and screw systems using a mini-swine craniomaxillofacial Osteotomy fixation model. Journal of oral and maxillofacial surgery : official journal of the American Association of Oral and Maxillofacial Surgeons 76 (10), 2138–2150.
Schwartz-Dabney, C.L., Dechow, P.C., 2003. Variations in cortical material properties throughout the human dentate mandible. Am. J. Phys. Anthropol. 120 (3), 252–277.
Staiger, M.P., Pietak, A.M., Huadmai, J., Dias, G., 2006. Magnesium and its alloys as orthopedic biomaterials: a review. Biomaterials 27 (9), 1728–1734.
Steffen, C., Sellenschloh, K., Vollmer, M., Morlock, M.M., Heiland, M., Huber, G., Rendenbach, C., 2020. Biomechanical comparison of titanium miniplates versus a variety of CAD/CAM plates in mandibular reconstruction. J. Mech. Behav. Biomed. Mater. 111, 104007.
Steffen, C., Fischer, H., Sauerbrey, M., Heintzelmann, T., Voss, J.O., Koerdt, S., Checa, S., Kreutzer, K., Heiland, M., Rendenbach, C., 2022. Increased rate of pseudarthrosis in the anterior intersegmental gap after mandibular reconstruction with fibula free flaps: a volumetric analysis. Dentomaxillofacial Radiol. 51 (7), 20220131.
Turostowski, M., Rendenbach, C., Herzog, P., Ellinghaus, A., Prates Soares, A., Heiland, M., Duda, G.N., Schmidt-Bleek, K., Fischer, H., 2024. Titanium vs PEO surface-modified magnesium plate fixation in a mandible bone healing model in sheep. ACS Biomater. Sci. Eng. 10 (8), 4901–4915.
Wang, J.L., Xu, J.K., Hopkins, C., Chow, D.H., Qin, L., 2020. Biodegradable magnesium-based implants in Orthopedics-A general review and perspectives. Adv. Sci. (Weinh.) 7 (8), 1902443.
Witte, F., 2010. The history of biodegradable magnesium implants: a review. Acta Biomater. 6 (5), 1680–1692.
Zhao, D., Witte, F., Lu, F., Wang, J., Li, J., Qin, L., 2017. Current status on clinical applications of magnesium-based orthopaedic implants: a review from clinical translational perspective. Biomaterials 112, 287–302.